PRELIMINARY LANGMUIR PROBE ANALYSIS FROM ESPRIT

Adam C. Escobar, Sven G. Bilén, and C. Russell Philbrick

The Pennsylvania State University, Electrical Engineering Department, University Park, PA 16802, USA
Email: ace128@psu.edu, sbilen@psu.edu, crp3@psu.edu

ABSTRACT

On 1 July 2006, the ESPRIT sounding rocket launched several student-built scientific instruments from Andøya Rocket Range in Norway. Two of the instruments had the objective of characterizing the plasma environment: Langmuir probes and a plasma frequency probe. This paper presents a brief overview of the ESPRIT mission, but focuses mostly on the analysis of the Langmuir probes experiment. The Langmuir probes experiment included one swept-bias probe and one fixed-bias probe, both radial to the payload axis. Comparisons between datasets from the Langmuir probes and the ground-based instruments are emphasized. A preliminary investigation of the Langmuir probe data shows several interesting features. The scientific measurements include the presence of a noctilucent cloud (NLC), polar mesospheric summer echo (PMSE), and a sporadic-*E* layer.

1. MISSION OVERVIEW

The ESPRIT sounding rocket was launched at 06:39.00 UTC on 1 July 2006 from Andøya Rocket Range in Norway. The primary mission of ESPRIT was to investigate the mesosphere and ionosphere in the high latitude regions. The measurements were conducted during a time when NLCs, PMSEs, and sporadic-*E* layers were present.

Two of the instruments had the objective of characterizing the plasma environment: Langmuir probes and a plasma frequency probe. The plasma frequency probe data currently needs further analysis to understand those data, and it will not be explained in the scope of this manuscript. The goal of the plasma frequency probe was to demonstrate a new measurement capability.

The payload was spin-stabilized at a rate of approximately 5.45 Hz, and it reached an apogee of approximately 169 km. During the mission a NLC layer, a double-layer PMSE, and a sporadic-*E* Layer were present. Several ground based instruments recorded data during the launch; these included the RMR Lidar, ALWIN (VHF), Tromsø Digisonde, EISCAT VHF, and EISCAT UHF radars.

2. LANGMUIR PROBE INSTRUMENT

2.1. Physical Design

The Langmuir probes were designed such that orbital motion limited (OML) analysis could be employed, i.e., the probe radius was much smaller than the Debye length. The experiment included two cylindrical tri-axial probes radial to the payload axis (see Fig. 1). The probes were of similar geometry to the probes used by L. Brace on *Dynamics Explorer 2* and the *Pioneer Venus Orbiter* [1]. Only the probe radius was changed due to the longer Debye length in our case. The probes were composed of brass with thin gold plating to minimize the photoelectric current.

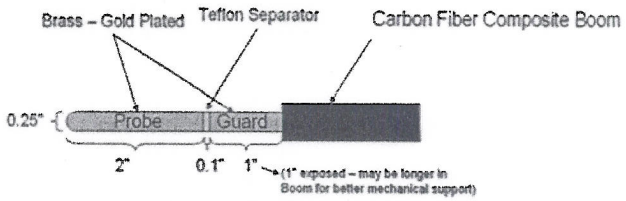

Figure 1. ESPRIT Langmuir probe geometry.

The probes were attached at the end of a double-hinged boom system on the forward bulkhead underneath the nosecone, as shown in Fig 2. The boom length agrees with previously suggested lengths of 0.3 to 1.0 m [1] to be outside the rocket's perturbing effects.

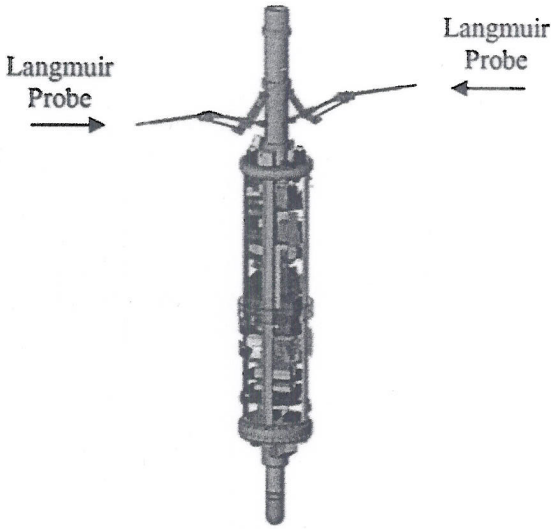

Figure 2. ESPRIT internal components.

Proc.18th ESA Symposium on 'European Rocket and Balloon Programmes and Related Research', Visby, Sweden, 3-7 June 2007 (ESA SP-647, November 2007)

2.2. Electronic Design

The electrometer design was based upon a fixed-gain logarithmic amplifier. RFI filters were used for all inputs and outputs to reduce radio frequency interference (RFI). The gain allowed a current range of 0.1 nA to 50 μA.

The swept-bias voltage was created for one of the elements from a microcontroller and digital-to-analog converter. The swept-bias function was a sawtooth waveform sweeping from −10 V to +10 V at a rate of 1 Hz. The second probe used a fixed-bias voltage that was implemented by a precision +5-V voltage reference.

The electrometer gain was selected to provide an output with the desired resolution of the data. The design included multiple windowing stages for different gains. The output of the experiment was an analog signal from 0 V to +5 V, and it was transferred to the telemetry system for digital processing and transmission.

3. PRELIMINARY ANALYSIS

The data analysis utilized the OML approach, which is employed when the probe radius is much smaller than the Debye length. Using this approach, the plasma potential, electron density, electron temperature, and ion density can be found. The swept-bias probe provides data for all four of these plasma characteristics. The fixed-bias probe was set at a positive voltage in the electron saturation range (at +5 V); therefore, this probe provides high temporal and, hence, spatial resolution measurements of electron density.

3.1. Plasma Potential

Using the swept-bias probe data, the current versus voltage curve (*I–V* curve) determines the plasma potential. Fig. 3 depicts the ideal *I–V* curve shape. The voltage at the inflection point that separates the electron retardation region and electron saturation region determines the plasma potential. The potential with respect to the spacecraft ground is the plasma potential. This voltage is positive, which indicates that the spacecraft is negative with respect to the plasma. The payload charges negative relative to the plasma because of the easier collection of free electrons. Exposed voltages can also affect the spacecraft potential.

In finding the inflection point of the *I–V* curve, the data having negative current values were omitted, and then a third-order polynomial was fitted to the remaining curve. The second derivative of this function is used to determine the inflection point. Fig. 4 illustrates the upleg and downleg plasma potential relative to the spacecraft. Both graphs are similar, indicating the upleg and downleg potential agree for the plasma conditions around the payload as a function of altitude.

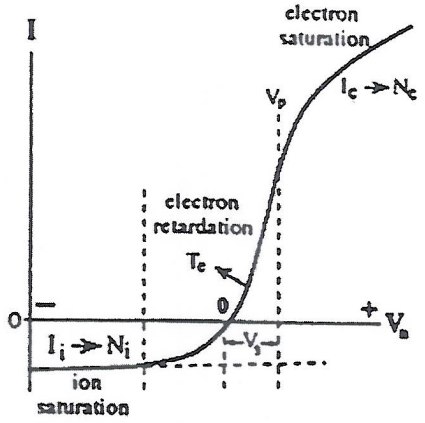

Figure 3. Langmuir probe I–V *relationship [1]*

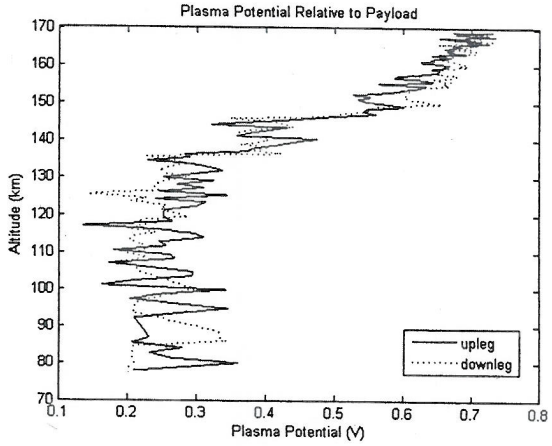

Figure 4. Upleg and downleg plasma potential.

3.2. Electron Density

The swept- and fixed-bias probes measure the electron density by using the electron saturation region of the *I–V* curve. Thus, for the swept-bias probe, the temporal resolution of the electron density is much lower than that of the fixed-bias probe data; hence, that probe's data was used for increased spatial resolution.

In order to find the electron density, the relationship between the probe current and voltage as a function of the electron density is needed. The equation for the electron saturation current is given by the relationship,

$$I_e = \frac{2N_e Ae}{\sqrt{\pi}} \sqrt{\frac{kT_e}{2\pi m_e}} \sqrt{1 + \frac{e(V_{probe} - V_{plasma})}{kT_e}}, \quad (1)$$

where

N_e = electron density
A = surface area of probe
e = electron charge
k = Boltzmann constant
T_e = electron temperature

m_e = electron mass
V_{probe} = probe potential respect to spacecraft
V_{plasma} = plasma potential respect to spacecraft

Since a cylindrical probe was used, the electron temperature, T_e, measurements are not necessary to obtain electron density measurements [1]. The reason for this is due to the fact that

$$\frac{e(V_{probe} - V_{plasma})}{kT_e} >> 1. \quad (2)$$

For these measurement conditions, the kT_e terms cancel out, and the resulting equation for the electron density is

$$N_e = \frac{\pi I_e}{Ae}\sqrt{\frac{m_e}{2e(V_{probe} - V_{plasma})}}. \quad (3)$$

Using Eq. 3, Fig. 5 shows the results from the upleg electron density profile measured by ESPRIT. Two noticeable features are the electron density depletion in the NLC layer and the electron density enhancement in the sporadic-*E* layer.

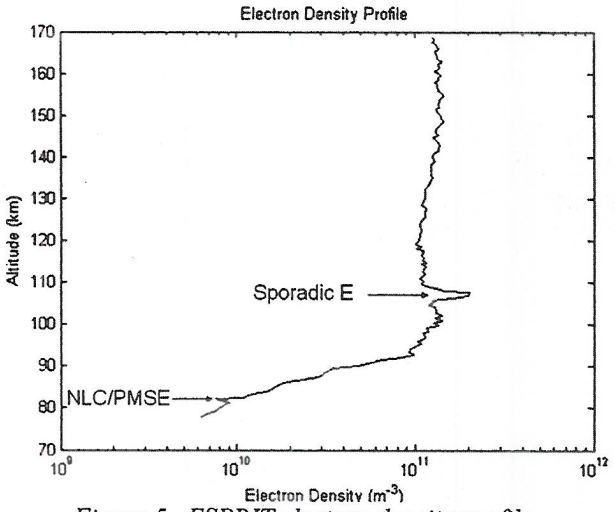

Figure 5. ESPRIT electron density profile.

The NLC layer was in the altitude range of 81.6 km to 83.8 km (as measured by ALOMAR RMR Lidar). The dual-band PMSE layers have ranges: 82.5 km to 84.4 km for the lower band and 86.3 km to 90.0 km for the upper band (measured by the ALWIN VHF Radar). The NLC layer is slightly below the PMSE layers, and lies partially within the lower PMSE layer. A minimum occurs in electron density at the NLC layer; it was 6.5×10^9 m^{-3} at an altitude of 82.1 km in the NLC layer.

The sporadic-*E* layer exhibited an electron density of 2.35×10^{11} m^{-3} at an altitude of 107.0 km. The electron density profile measured by ESPRIT agrees reasonably well with the ground-based measurements from the EISCAT radar. Fig. 6 shows closer agreement between the probe and the UHF radar, which was pointed toward the rocket launch area, than with the vertically pointed VHF radar located at Tromsø. The Langmuir probe measurements were found by using Langmuir theory as indicated above. The profile found did not need to be normalized and adjusted to an existing reference.

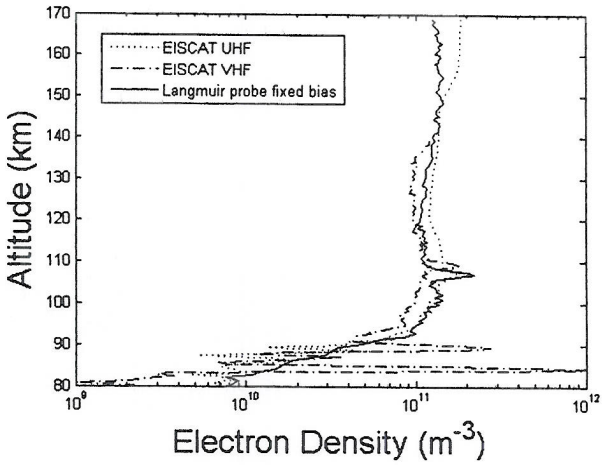

Figure 6. ESPRIT and ground-based electron density profiles (EISCAT Radar courtesy of Magnar G. Johnsen, University of Tromsø, see [2]).

3.3. Electron Temperature

The electron temperature is found using the swept-bias probe data. The slope of the electron retardation region is used to determine the electron temperature. The equation for current in the electron retardation region is given as

$$I_e = eN_e\sqrt{\frac{kT_e}{2\pi m_e}}\cdot\exp^{\frac{e(V_{probe} - V_{plasma})}{kT_e}}. \quad (4)$$

Eq. 4 can be reduced further by taking the natural logarithm of both sides and differentiating with respect to the potential of the probe in the plasma, which yields

$$T_e = \frac{e}{k}\cdot\frac{1}{\frac{d}{dV_{probe}}[\ln(I_e)]}. \quad (5)$$

The term $d[(\ln(I_e))]/dV_{probe}$ in Eq. 5 is the slope of the electron retardation region. By taking the natural log of the current values and relating these values to the probe potential voltage with respect to the plasma, a linear fit can determine the value of the slope and, hence, the electron temperature can be found from Eq. 5.

The electron temperature analysis for ESPRIT is still under investigation. Preliminary analysis depicts a

change in the *I–V* slope from a steep slope at lower altitudes to a larger slope at higher altitudes, suggesting a change from lower temperatures to higher temperatures. At lower altitudes, determining temperatures with Langmuir probes (especially below 300 K) has been found to be difficult. Temperature measurements below this range have been found to have larger errors due to work function patchiness [1, 3].

3.4. Mean Ion Density

Using the ion saturation region, the mean ion density was found. The equation to determine the collector ion current in the ion saturation region is given as

$$I_i = \frac{AeN_i v_i}{\pi}\sqrt{1+\frac{kT_i}{m_i v_i^2}+\frac{2e\left(V_{\text{probe}}-V_{\text{plasma}}\right)}{m_i v_i^2}}, \qquad (6)$$

and solving for mean ion density, N_i, yields

$$N_i = \frac{\pi I_i}{Ae}\sqrt{\frac{m_i}{m_i v_i^2 + kT_i + 2e\left(V_{\text{probe}}-V_{\text{plasma}}\right)}}. \qquad (7)$$

To calculate the mean ion density, certain assumptions were taken into consideration regarding the mean ion velocity (v_i), mass (m_i), and temperature (T_i). The mean ion velocity was approximated by the rocket's velocity. However, this will result in errors near apogee because the mean ion velocity is greater than the payload velocity there. The mean ion mass was taken to be 26 amu to account for the abundance of NO^+, O_2^+, and O^+ ions. The ion temperature profile is expected to be similar to the electron temperature profile at lower altitudes where the collision frequency is high [4, 5, 6].

4. ANOMALOUS FEATURES

There are four anomalous features in the Langmuir probe data analysis: upleg and downleg disagreement, swept-bias probe interference, mean ion and electron density disagreement, and *I–V* curve shifts.

4.1. Upleg and Downleg Disagreement

The upleg and downleg data for both probes disagree greatly in magnitude. Fig. 7 displays the unfiltered fixed-bias probe on upleg and downleg, with current plotted as a function of altitude. The downleg current is almost an order of magnitude lower than the upleg current. The explanation is the shadowing of the probes in the payload's wake. Fig. 7 also shows a diagram of the payload's trajectory. The affected data actually starts near apogee, where the velocity of the payload has mostly a horizontal velocity component, and the probes spin in and out of the payload's wake. This shadowing effect in the data then continues throughout the entire downleg.

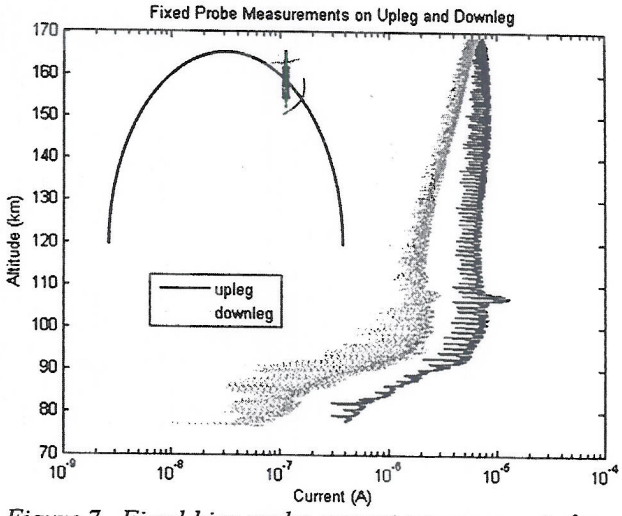

Figure 7. Fixed-bias probe current measurements from upleg and downleg.

4.2. Swept-Bias Probe Interference

The swept-bias probe created interference on two other instruments aboard ESPRIT; the fixed-bias Langmuir probe and the aerosol detector. Swinging the probe potential from −10 V to +10 V, with respect to the payload, changes the vehicle potential. This change in the payload potential can be seen in the fixed-bias probe data and the aerosol detector data. The one-second (1-Hz) periodic sweep of the probe alters the fixed-bias probe data on each sweep, as seen in Fig. 8. However, most of the fixed-bias probe data is still valid. The data was valid only when the swept-bias probe was negative or near zero with respect to the rocket. In order to filter out the invalid data, sections of the fixed-bias probed data measured during the positive sweep were omitted in creating the final electron density plot shown in Fig. 5.

A solution to preventing this interference, or at least decreasing the effect, is to sweep over a lower voltage range. A suggested sweep range would be from −5 V to +5 V. One consideration in this case is that the rather large face of the aerosol detector exposed a +6-V grid that was intended to deflect ambient ions. The electron collection on this aperture grid would certainly have a significant effect on the vehicle potential. An added feature would be to have a "rest period" once the probe's voltage reached these minimum and maximum values. During the ESPRIT mission, when the swept-bias probe transitioned from positive +10 V to −10 V, there was a capacitive response that created invalid data. Having a rest period at the minimum and maximum ranges would allow valid data during the transition.

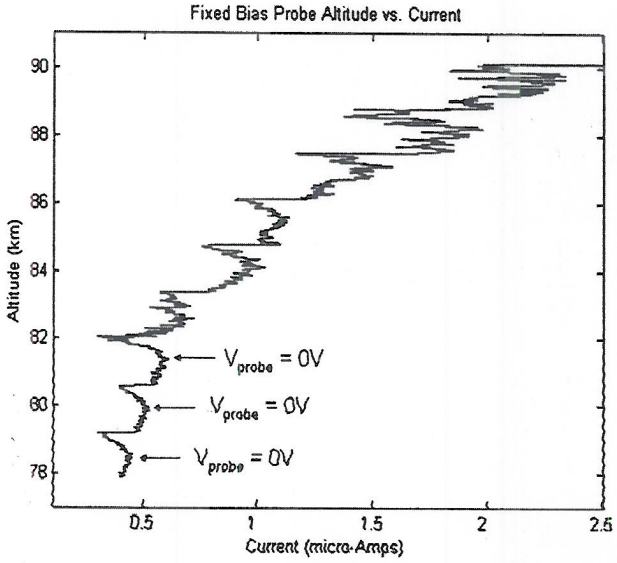

Figure 8. Swept-bias probe influence on the fixed-bias probe current collection.

4.3. Mean Ion and Electron Density Disagreement and *I–V* Curve Shifts

In an ideal ionosphere, the positive ion density and electron density are expected to be of similar magnitude above 90 km. During the ESPRIT mission, there is a large disagreement between the mean ion density and the electron density below 105 km, which continues through the NLC layer and the region from 90 km to 100 km, where the mean ion density is much larger than the electron density. Fig. 9 shows the measured ion density and electron density profiles as a function of altitude, and the ionospheric features discussed previously are also labeled on this figure.

The electron density plot in the NLC layer depicts a decrease in electron density, and the ion density plot in the NLC layer illustrates an ion enhancement. These features have been previously observed in the *D*-region during NLC conditions during the CAMP campaign [7]. The electron density is thought to decrease in the region of the NLC as electrons collide with and attach to the ice particles [7]. The same reason would result in the positive ion enhancement in the NLC layer since the ion–electron recombination loss would be reduced.

The cause of the ion density enhancement from 90 km to 100 km is still under investigation. The density disagreement is almost an order of magnitude. The readings suggest an abundance of positive ions. The region where this anomaly occurs is between the top of the PMSE band (at 90.0 km) and the sporadic-*E* layer (at 107.0 km). An *I–V* curve shift is associated with this ion enhancement region from 90.0 km to 100.0 km. The shift in the *I–V* curve with respect to the spacecraft ground is shown in Fig. 10.

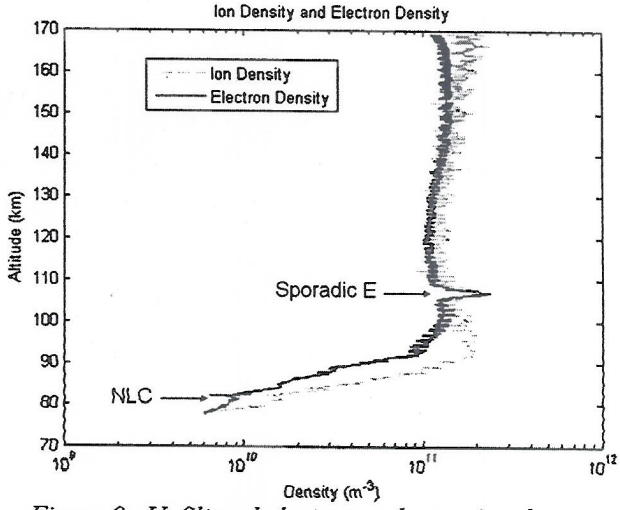

Figure 9. Unfiltered electron and mean ion density profiles.

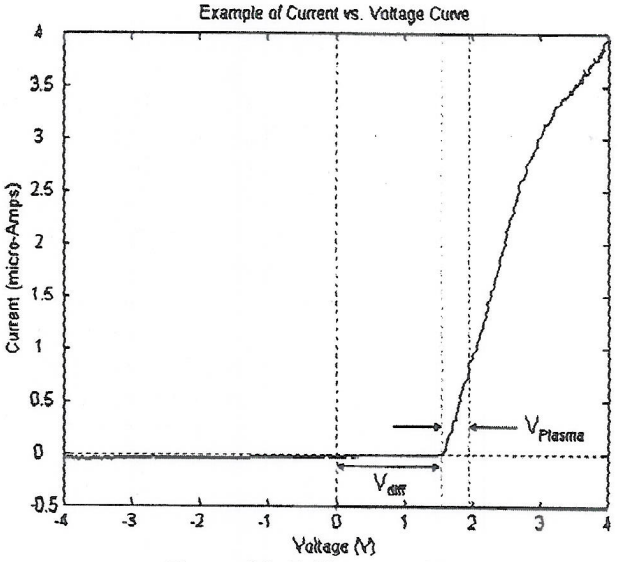

Figure 10. I–V curve shift.

The rocket "ground" potential should be near the point where the current changes from a negative value to a positive value; however, this was not the case. The change in spacecraft ground was analyzed and plotted with respect to mission time in Fig. 11. This voltage difference changed rapidly when the payload entered the upper band of the PMSE layer that was located between 86.3 km and 90.0 km. The analysis of the charge collection to the vehicle is continuing.

5. SUMMARY AND CONCLUSIONS

The ESPRIT Langmuir probe instrument was successful in measuring the density profiles and illustrating the different mesospheric and ionospheric features during the mission. The electron density plot observed an electron depletion in the NLC layer and electron enhancement in the sporadic-*E* layer. The ion density

profile showed ion enhancements in the NLC layer and the sporadic-*E* layer. There was a disagreement between the electron and ion densities measured between the upper PMSE layer and sporadic-*E* layer. However, it is interesting to note that the electron density calculated using the probe geometry, without any adjustments, agrees very well with the EISCAT radar measurements shown in Fig. 6.

If Langmuir probes are mounted in the forward section of a payload, and with no attitude control system (similar to the ESPRIT Langmuir probe experiment), then there is expected to be invalid data on the downleg due to spacecraft wake effects. This should be considered when planning a mission.

To reduce swept-bias probe interference, a probe should sweep at a lower voltage range and add a resting period. This lower voltage range will result in a smaller effect upon the spacecraft potential, and the resting period will help provide valid data.

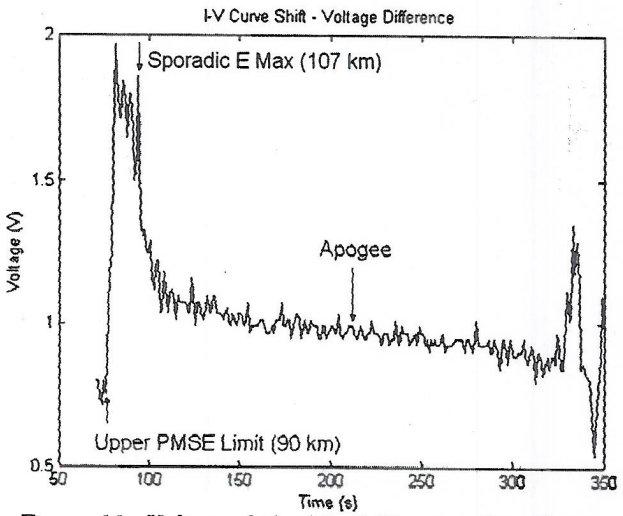

Figure 11. Voltage shift of the I–V curve plotted over mission time.

6. ACKNOWLEDGEMENTS

The fellow members of the ESPRIT team helped make this experiment possible; together with support from Penn State faculty advisors, Tim Wheeler, Russell Philbrick, Sven Bilén, Charles Croskey, John Mitchell, and Ram Narayanan. The launch operations were supported by the NASA Sounding Rocket Operations Contract, NASA Wallops Flight Facility, Andøya Rocket Range, ALOMAR Observatory, EISCAT Radar, and the Leibniz Institute of Atmospheric Physics. Institution sponsorship by the Penn State College of Engineering with particular support from the Electrical and Aerospace Engineering Departments, the University of Tromsø and Tromsø Geophysical Observatory, the University of Bergen, and the Technical University of Narvik are gratefully acknowledged. Funding from the Pennsylvania Space Grant Consortium through NASA's National Space Grant Consortium and Fellowship program, and from several corporate sponsors listed at http://spirit.ee.psu.edu/spiritiii/Sponsors.htm made this project possible.

7. REFERENCES

1. Brace, Larry H., "Langmuir Probe Measurements in the Ionosphere," in *Measurement Techniques in Space Plasmas: Particles*, American Geophysical Union: Monograph 102, 1998.
2. Edwards, Perry S., C. Russell Philbrick, Magnar G. Johnsen, Ralph Latteck, Gerd Baumgarten, C. Russell Philbrick, Magnar G. Johnsen, Ralph Latteck, Gerd Baumgarten, "Polar Atmospheric Measurements Confirmed Through ESPRIT Rocket Payload Launch," Ibid.
3. Hoegy, Walter R., and Brace, Larry H., "Use of Langmuir Probes in non-Maxwellian Space Plasmas," *Review of Scientific Instruments*, Vol. 70, No. 77, pp. 3015–3024, 1999.
4. Jursa, Adolph S., *Handbook of Geophysics and the Space Environment*, Chapters 9 and 10, Air Force Geophysics Laboratory, 1985.
5. Schunk, Robert W., and Nagy, Andrew F., *Physics, Plasma Physics, and Chemistry*, Cambridge University Press: Cambridge, U.K., 2000.
6. Tascione, Thomas, *Introduction to the Space Environment*, Krieger Publishing Company: Malabar, Florida, 1994.
7. Kopp, E., Bertin, F., Bjorn, L.G., Dickinson, P.H.G., Philbrick, C.R., and Witt, G., "The 'Camp' Campaign 1982," *Proceed. 7th ESA Symp.*, ESA SP-229, pp. 117–123, 1985.